Synaptic influences on rat ganglion-cell photoreceptors

Kwoon Y. Wong, Felice A. Dunn, Dustin M. Graham and David M. Berson

Department of Neuroscience, Brown University, Box G-L471, Providence, RI 02912, USA

The intrinsically photosensitive retinal ganglion cells (ipRGCs) provide a conduit through which rods and cones can access brain circuits mediating circadian entrainment, pupillary constriction and other non-image-forming visual functions. We characterized synaptic inputs to ipRGCs in rats using whole-cell and multielectrode array recording techniques. In constant darkness all ipRGCs received spontaneous excitatory and inhibitory synaptic inputs. Light stimulation evoked in all ipRGCs both synaptically driven ('extrinsic') and autonomous melanopsin-based ('intrinsic') responses. The extrinsic light responses were depolarizing, about 5 log units more sensitive than the intrinsic light response, and transient near threshold but sustained to brighter light. Pharmacological data showed that ON bipolar cells and amacrine cells make the most prominent direct contributions to these extrinsic light responses, whereas OFF bipolar cells make a very weak contribution. The spatial extent of the synaptically driven light responses was comparable to that of the intrinsic photoresponse, suggesting that synaptic contacts are made onto the entire dendritic field of the ipRGCs. These synaptic influences increase the sensitivity of ipRGCs to light, and also extend their temporal bandpass to higher frequencies. These extrinsic ipRGC light responses can explain some of the previously reported properties of circadian photoentrainment and other non-image-forming visual behaviours.

(Resubmitted 30 March 2007; accepted after revision 10 May 2007; first published online 17 May 2007)
Corresponding author K. Y. Wong: Department of Neuroscience, Brown University, Box G-L471, Providence, RI 02912, USA. Email: kwoon_wong@brown.edu

A rare type of mammalian retinal ganglion cell is directly light responsive (Berson *et al.* 2002; Sekaran *et al.* 2003; Warren *et al.* 2003). These intrinsically photosensitive retinal ganglion cells (ipRGCs) express melanopsin (Provencio *et al.* 1998, 2002; Gooley *et al.* 2001; Hannibal & Fahrenkrug, 2002; Hannibal *et al.* 2002; Hattar *et al.* 2002, 2003; Lucas *et al.* 2003), which binds retinaldehyde to form their photopigment (Newman *et al.* 2003; Fu *et al.* 2005; Melyan *et al.* 2005; Panda *et al.* 2005; Qiu *et al.* 2005). The intrinsic light responses of ipRGCs are less sensitive and more sluggish than those of rods and cones, but tonically encode the intensity of bright environmental illumination (Berson *et al.* 2002; Dacey *et al.* 2005). Axons of ipRGCs innervate the suprachiasmatic nucleus (SCN), where they contribute to the photic entrainment of circadian rhythms (Gooley *et al.* 2001, 2003; Hannibal & Fahrenkrug, 2002; Hannibal *et al.* 2002; Hattar *et al.* 2002, 2003; Panda *et al.* 2002, 2003; Ruby *et al.* 2002; Rollag *et al.* 2003; Semo *et al.* 2003; Warren *et al.* 2003). They also project to the olivary pretectal nucleus (OPN), where they participate in the pupillary light reflex (Lucas *et al.* 2001, 2003; Gooley *et al.* 2003; Hattar *et al.* 2003; Panda *et al.* 2003).

Though ipRGCs can function as photoreceptors, they are also subject to intraretinal synaptic influences. Their extensive dendritic arbours, which serve in part as sites of phototransduction (Berson *et al.* 2002; Hannibal & Fahrenkrug, 2002; Hattar *et al.* 2002; Provencio *et al.* 2002), are deployed in the inner plexiform layer (IPL), the synaptic layer in which bipolar and amacrine cells convey rod and cone signals to ganglion cells (Berson *et al.* 2002; Hannibal *et al.* 2002; Hattar *et al.* 2002; Provencio *et al.* 2002; Belenky *et al.* 2003). Indeed, Belenky *et al.* (2003) used electron microscopy to identify synaptic contacts from both amacrine cells and presumed ON bipolar cells onto melanopsin-immunopositive processes in the IPL of the mouse retina. In primate and rat ipRGCs, light evokes not only the intrinsic, melanopsin-based response but also synaptically mediated signals originating in rods and cones (Dacey *et al.* 2005; Perez-Leon *et al.* 2006). The ipRGCs may therefore constitute a critical node in polysynaptic circuits linking rods and cones to the SCN, OPN and related nuclei, and thus play a key role in the influence of these conventional photoreceptors upon non-image-forming photic responses (Aggelopoulos & Meissl, 2000; Ruby *et al.* 2002; Panda *et al.* 2002, 2003; Hattar *et al.* 2003; Lucas *et al.* 2003; Mrosovsky & Hattar, 2003).

The goal of this study was to provide a more complete electrophysiological picture of the synaptic influences impinging on ipRGCs. We sought to identify which

 DOI: 10.1113/jphysiol.2007.133751

classes of retinal cells provide the input, and how light responses mediated by synaptic inputs differ functionally from those based on endogenous phototransduction. We conducted our studies in rats, in part because this and other rodent species are favoured models for studying ipRGCs and non-image-forming visual functions. We find that all ipRGCs receive synaptic inputs involving fast neurotransmitters, both excitatory (glutamate) and inhibitory (GABA and glycine). These synaptic inputs are spontaneously active and can also be triggered by light. These extrinsic light responses are transient near threshold but appear fairly sustained in response to brighter light. They are carried primarily through the ON channel via ON bipolar and amacrine cells, although a very weak input from OFF bipolar cells also exists. The ON bipolar cell input appears to be made onto the entire dendritic field of the ipRGCs. These synaptic inputs permit ipRGCs to respond to temporal frequencies higher than are resolvable by the intrinsic photosensory mechanism and provide a basis for rods and cones to regulate non-image-forming visual centres. Some of these results appeared previously in abstract form (F.A.D. and D.B., *Association for Research in Vision & Ophthalmology*, 2002; K.Y.W. and D.B., ibid, 2005).

Methods

Animals

The experiments were performed on a total of 120 adult Sprague-Dawley rats (Charles River, Wilmington, MA, USA). All procedures conformed to National Institutes of Health guidelines for work with laboratory animals and were approved by the Institutional Animal Care and Use Committee at Brown University.

Whole-cell recording

Retrograde labelling. Male rats 56–70 days of age were anaesthetized with ketamine (60 mg kg^{-1} I.P. Wyeth, Madison, NJ, USA) and medetomidine (0.4 mg kg^{-1} I.P.; Orion Corporation, Finland). Rhodamine-labelled fluorescent latex microspheres (0.1–0.3 μl; Lumafluor; Naples, FL, USA) were deposited stereotaxically into the hypothalamus unilaterally through glass pipettes tilted 10 deg from vertical.

***In vitro* preparation and recording.** Five to 60 days after tracer injection, animals were killed with Beuthanasia (360 mg kg^{-1} I.P.; Schering-Plough Animal Health, Union, NJ, USA) or carbon dioxide, and the eyes were removed and hemisected under ambient white room light. After removal of the vitreous humour, eyecups were kept in dim red light and maintained at room temperature (20–25°C) in bicarbonate-based Ames' medium gassed with 95% O_2 5% CO_2 before being transferred to a recording chamber. Flattened eyecups were mounted on a coverslip with the vitreal surface up, anchored by a weighted nylon mesh, and placed in a chamber (Warner RC-26GLP; Hamden, CT, USA). The chamber was mounted on a fixed-stage upright microscope (Nikon E600FN; Melville, NY, USA). Retrolabelled RGCs were located by epifluorescence (530–550 nm, 5.1×10^{17} photons cm^{-2} s^{-1}). Following mechanical exposure of the soma using an empty patch pipette, whole-cell patch recordings were established using pipettes pulled from thick-walled borosilicate tubing (tip resistances 4–7 MΩ) on a Flaming/Brown P-97 puller (Sutter Instruments, Novato, CA, USA). Recordings were made with a Multiclamp 700A amplifier (Axon Instruments, Union City, CA, USA). Electrode capacitance and series resistance were partially compensated, and the remaining series resistance was typically around 10–25 MΩ. pCLAMP 9 software (Axon Instruments) was used for data acquisition. Signals were low-pass filtered (200 Hz to 4 kHz cutoff), and the sampling frequency was at least four times the low-pass filter cutoff. Liquid junction potentials (14 mV for the K^+-based and 10 mV for the Cs^+-based internal solutions; see below) were corrected for all recordings. Voltage-ramp characterization of responses to puff-applied agonists was performed as previously described (Wong *et al.* 2005*a*).

Bathing and intracellular solutions. In experiments involving light responses, the bathing solution was bicarbonate-based Ames' medium gassed with 95% O_2 5% CO_2 and maintained at 32–34°C with a temperature controller (ATR-4, Quest Scientific, Canada). In the puffing experiments, the Ringer contained (mM): 120 NaCl, 3.1 KCl, 0.5 KH_2PO_4, 1.24 $MgSO_4$, 10 Hepes, 2 $CoCl_2$, 0.5 L-glutamine, 0.0005 tetrodotoxin (TTX), and 40 D-glucose, and was adjusted to pH 7.4 with NaOH. This Hepes-based Ringer was maintained at room temperature and not gassed. Intracellular solutions contained (mM): 120 potassium gluconate or Cs-methanesulphonate, 5 NaCl, 4 KCl or CsCl, 10 Hepes, 2 EGTA, 4 Mg-ATP, 0.3 Na-GTP, and 7 $Tris_2$-phosphocreatine, and were adjusted to pH 7.3 with KOH or CsOH. The potassium-based solution was used in current-clamp experiments, whereas the caesium-based solution was used in voltage-clamp experiments to improve space clamp. In the voltage-clamp experiments shown in Figs 2, 3, 7 and 8*A*, 1 mM QX-314 chloride was also added to the intracellular solution, and the calculated Nernst potentials for chloride are −64.2 mV at 20°C and −67.3 mV at 34°C. The bathing solutions were gravity fed into the recording chamber at 2–4 ml min^{-1}.

Light stimuli. Light stimuli were full-field, broadband white light. Neutral density filters (Newport/Oriel,

Stratford, CT, USA) were used to control stimulus energy. Except for the experiment shown in Fig. 12, all light flashes were presented with interstimulus intervals ranging from 2 min (for the lowest intensities) to 10 min (for the highest intensities) to allow the cell to recover from the previous flash. Light stimuli were introduced from below through the recording chamber's glass bottom, using the microscope's 100 W tungsten-halogen lamp and transillumination optics. The irradiance of unattenuated stimulus light (i.e. 0 log I) at the ganglion cell layer was 2.3×10^{13} photons cm^{-2} s^{-1} sampled at 480 nm (see Wong *et al.* 2005*b* for methods). A logic-controlled electromechanical shutter regulated stimulus timing.

Multi-electrode array (MEA) recording

***In vitro* preparation and recording.** Rats of either sex and at least 50 days of age were used in these experiments. Animals were dark-adapted overnight and killed under dim red light with carbon dioxide or Beuthanasia. Eyes were removed and hemisected. Retinas were isolated from the eyecups with a paint brush and kept in bubbled Ames' medium at room temperature. Each retina was cut into two halves. One of these was flattened and placed ganglion-cell side down on a MEA; the other half was discarded. The MEA contained 60 electrodes, each 30 μm in diameter, at a centre-to-centre spacing of 200 μm (Multi Channel Systems, Germany). The retina was continuously superfused at 2 ml min^{-1} with bicarbonate-based Ames' medium gassed with 95% O_2 5% CO_2 and maintained at 32–34°C with a temperature controller (TC-324B, Warner Instruments, Hamden, CT, USA), and was kept in darkness except when stimulated by light. Presentation of light stimuli started after the preparation had been superfused for 1 h. Spiking activity was amplified, filtered (cutoffs at 200 Hz and 3 kHz) and digitized at 25 kHz using MC Rack software (Multi Channel Systems). Cluster analysis of the spike data was performed using Offline Sorter software (Plexon Inc., Dallas, TX, USA). All data derived from these experiments were drawn from single cells whose spike amplitudes were at least 50% larger than both the noise level and the next largest spike. All ipRGCs were identified based on their ability to generate sluggish, melanopsin-based responses to bright light in the presence of a pharmacological cocktail blocking rod/cone signalling (see below). The light responses of conventional RGCs were completely silenced by this cocktail.

Light stimuli. For full-field light stimulation, the light source was an FO-6000 tungsten-halogen lamp with a built-in logic-controlled electromechanical shutter and filter holder (World Precision Instruments, Sarasota, FL, USA). Full-field light stimuli were directed onto the retina by a fibre optics cable. The unattenuated intensity at the surface of the preparation was 3.8×10^{12} photons cm^{-2} s^{-1} sampled at 480 nm. The '+0.65 log' light intensity was generated by removing the filter holder and attaching the fibre optics cable directly to the lamp housing. Light flashes were presented with interstimulus intervals ranging from 2 min (for the lowest intensities) to 10 min (for the highest intensities), to allow the cells to recover from the previous flash.

For receptive field mapping, stimuli were generated by custom Flash MX software (Adobe, San Jose, CA, USA) and displayed through a digital DLP projector (Optoma EP719). The stimulus display, when focused onto the retinal surface with a pair of lenses, covered a 2.4 mm × 2.4 mm region. The MEA, which measured 1.4 mm on each side, was centred within this region. Stimulus intensity was adjusted by placing neutral-density filters in the light path.

To map the receptive field of the synaptically driven light response, a circular white spot (diameter: 120 μm; intensity: 8.4×10^8 photons cm^{-2} s^{-1} sampled at 480 nm) was presented sequentially at 400 different locations against a 'black' background (intensity = 3.8×10^5 photons cm^{-2} s^{-1} sampled at 480 nm). The spot appeared for 0.5 s at each location, and was presented at a new position every second. The sequence of spot locations followed the modified raster pattern illustrated in Fig. 1*A*. To estimate the area of the receptive field for each cell, we divided the retina into a two-dimensional grid, each square pixel (120 μm on each side) of which was centred on one of the spots in the stimulus sequence (Fig. 1*A*). We identified those pixels within which the stimulus spot evoked at least one spike (e.g. non-black pixels in Fig. 11*A*), and summed the area of these pixels. From this we calculated an equivalent diameter, corresponding to the diameter of a circle with the same total area.

For mapping the receptive field of the melanopsin-based light response, the retina was superfused with the rod/cone signalling blocker cocktail (see below). Because spots were ineffective in evoking the intrinsic response, the stimulus consisted of a bar (120 μm × 2400 μm; intensity = 2.1×10^{13} photons cm^{-2} s^{-1} sampled at 480 nm) presented against a 'black' background (intensity = 9.6×10^9 photons cm^{-2} s^{-1} sampled at 480 nm). The bar was presented at 20 different locations (Fig. 1*B*). It was illuminated for 19 s at each location and was presented at a new location every 75 s. The results from both types of mapping were plotted using Origin software (OriginLab, Northampton, MA, USA).

Chemicals

Chemicals were dissolved in distilled water to generate stock solutions, or dissolved directly into the internal or extracellular solution. To block transmission

of signals from conventional outer retinal photoreceptors to the inner retina, we blocked all bipolar cell light responses with a 'rod/cone signalling blocker cocktail' consisting of 100 μM L(+)-2-amino-4-phosphonobutyrate (L-AP4, a group III metabotropic glutamate receptor agonist), 40 μM 6,7-dinitroquinoxaline-2,3-dione (DNQX) or 6-cyano-7-nitroquinoxaline-2,3-dione (CNQX) (AMPA/kainate receptor antagonists), and 30 μM D-2-amino-5-phosphonovalerate (D-AP5) or 100 μM D-2-amino-7-phosphonoheptanoate (D-AP7) (NMDA receptor antagonists). To block amacrine cell signalling, we used, unless stated otherwise, an 'amacrine blocker cocktail' that included 30 μM (−)-bicuculline methochloride or 200 μM picrotoxin ($GABA_A$ receptor antagonists), 5 μM 3-[[(3,4-dichlorophenyl)methyl]amino]propyl] diethoxymethyl)phosphinic acid (CGP52432, $GABA_B$ receptor antagonist), 30–60 μM (1,2,5,6-tetrahydropyridin-4-yl)methylphosphinic acid (TPMPA, $GABA_C$ receptor antagonist), 5–10 μM strychnine (glycine receptor antagonist), 200–400 μM hexamethonium bromide (nicotinic acetylcholine receptor antagonist), 2–10 μM atropine (muscarinic acetylcholine receptor antagonist), and 500 nM TTX (voltage-gated sodium channel antagonist, to suppress spike-dependent synaptic release from amacrine cells). These blockers were bath-applied. For the agonist response experiments shown in Fig. 2, the agonists were locally puffed using a four-barrel puffer pipette with a combined tip diameter of 10–15 μm placed about 30 μm from the soma of the ipRGC being recorded. Puffing was controlled by an electronically regulated solenoid (Picospritzer, General Valve, Fairfield, NJ, USA). All drug effects were partially or fully reversible.

L-AP4, CNQX, DNQX, D-AP5, D-AP7, (−)-bicuculline methochloride and CGP52432 were purchased from Tocris (Ellisville, MO, USA), QX-314 chloride from Alomone (Israel), and TTX from Tocris, Sigma (St. Louis, MO, USA) and Biomol (Plymouth Meeting, PA, USA). All other chemicals were purchased from Sigma.

Results

ipRGCs express receptors for excitatory and inhibitory neurotransmitters

In all vertebrate retinas, conventional RGCs receive synaptic inputs from both bipolar and amacrine cells. To learn whether ipRGCs may be subject to such input, we first used voltage-clamp recordings to determine whether they possess receptors for the bipolar-cell transmitter glutamate, and the amacrine-cell transmitters GABA, glycine, and acetylcholine. We puffed receptor agonists onto ipRGCs and used baseline-subtracted voltage ramps to characterize the induced currents. To limit agonist effects to direct actions on the recorded

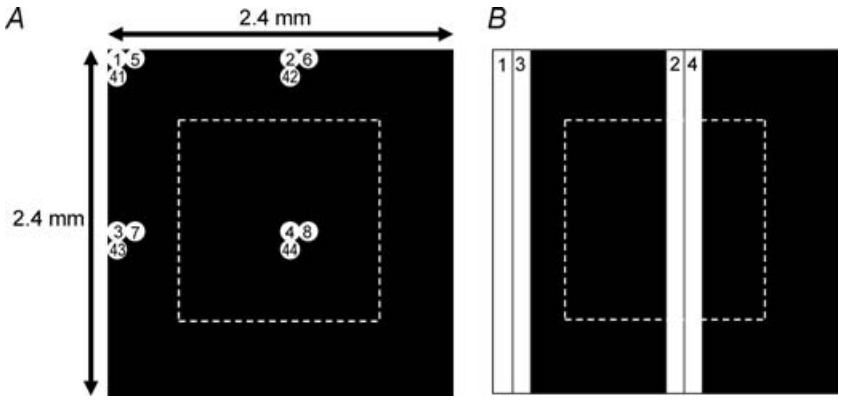

Figure 1. Stimuli used for mapping ipRGC receptive fields
A, stimulus configuration for mapping the extrinsic light response. A single circular white spot (120 μm diameter) was presented sequentially at 400 different locations within a square retinal region measuring 2.4 mm on each side. The MEA was positioned at the centre of this region (dotted outline). The 2.4 mm × 2.4 mm square was divided into quadrants, each further divided into 10 columns and 10 rows. In each cycle of stimulus presentation, the white spot was presented sequentially at the same relative location (i.e. same column and same row) within each quadrant. In the subsequent cycles, the spot was shifted to the adjacent column in the same row until it reached the right-hand boundary of that quadrant (10th column), then 'wrapped around' to the first column in the next row. In the diagram, the 1st, 2nd and 11th cycles of stimulus presentation are illustrated. The spots are shown to scale, with numbers indicating the serial order of spot presentation at that location. *B*, the stimulus for mapping the intrinsic light response. The same 2.4 mm × 2.4 mm square was divided into two halves, with each half subdivided into 10 columns. In each cycle of stimulus presentation, a 120 μm × 2400 μm white bar was illuminated sequentially at the same relative position in each half of the square. In the following cycle, the bar was shifted to the next column. The diagram illustrates the first two cycles of stimulation.

cell, we blocked calcium-mediated synaptic release by using a cobalt-based Ringer (see Methods). The caesium-based internal solution, which we used to improve space clamp, would have precluded our detecting any metabotropically mediated potassium conductances evoked by these agonists. All ipRGCs responded to applied L-glutamate with a current that was inward at negative holding potentials and reversed, on average, at -5.6 ± 0.3 mV (mean ± S.E.M.; $n = 15$; Fig. 2), near the cationic E_{rev}. Likewise, both GABA and glycine evoked currents in all ipRGCs tested and, as expected for fast ionotropic inhibitory currents, these reversed close to E_{Cl} (-57.3 ± 1.9 mV for GABA and -55.6 ± 0.9 mV for glycine; $n = 15$; Fig. 2). There were few if any nicotinic receptors on these cells, as neither acetylcholine (1 mM) nor the selective nicotinic agonist epibatidine (500 nM) evoked detectable currents ($n = 9$; not shown), although it should be noted that nicotinic receptors can desensitize rapidly and thus could have escaped detection. We conclude that ipRGCs possess the receptors for both excitatory bipolar-cell and inhibitory amacrine-cell transmitters.

Spontaneous synaptic inputs in darkness

To determine whether these receptors can be activated by synaptic input, we looked for spontaneous synaptic currents in cells bathed in a calcium-containing Ringer (Ames' medium) that permits synaptic transmission. In the absence of light stimulation, small spontaneous synaptic events could be observed under voltage clamp in all ipRGCs tested. These events reversed near -60 mV ($n = 17$; Fig. 3*A*). This is close to E_{Cl}, suggesting that, at rest, ipRGCs are bombarded by synaptic inputs that trigger inhibitory chloride conductances. To determine the transmitters mediating these inputs, we clamped ipRGCs close to the cationic E_{rev} to minimize glutamate-induced currents and to study the inhibitory ones in relative isolation. Subsequent application of antagonists of ionotropic GABA and glycine receptors induced a net inward current and a substantial reduction in synaptic noise ($n = 8$; Fig. 3*B*). We interpret this as a blockade of a large outward chloride conductance attributable to

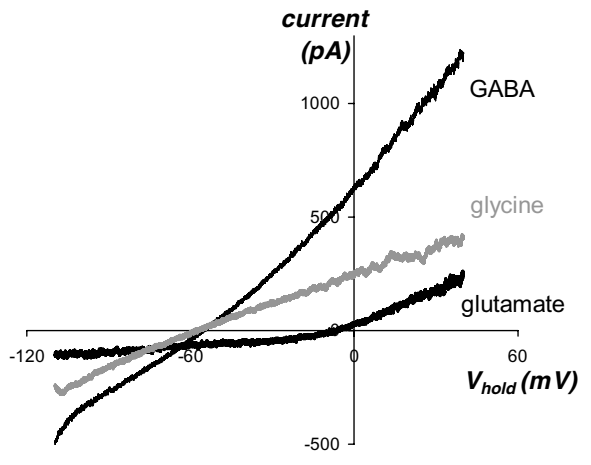

Figure 2. ipRGCs possess receptors for glutamate, GABA, and glycine
Responses of an ipRGC to exogenously applied neurotransmitter agonists. Synaptic transmission was blocked by extracellular cobalt. Ramp responses illustrate voltage dependence of baseline-subtracted currents evoked by puffed L-glutamate (2 mM, co-applied with 5 μM glycine as the co-agonist for NMDA receptors), GABA (1 mM), and glycine (1 mM).

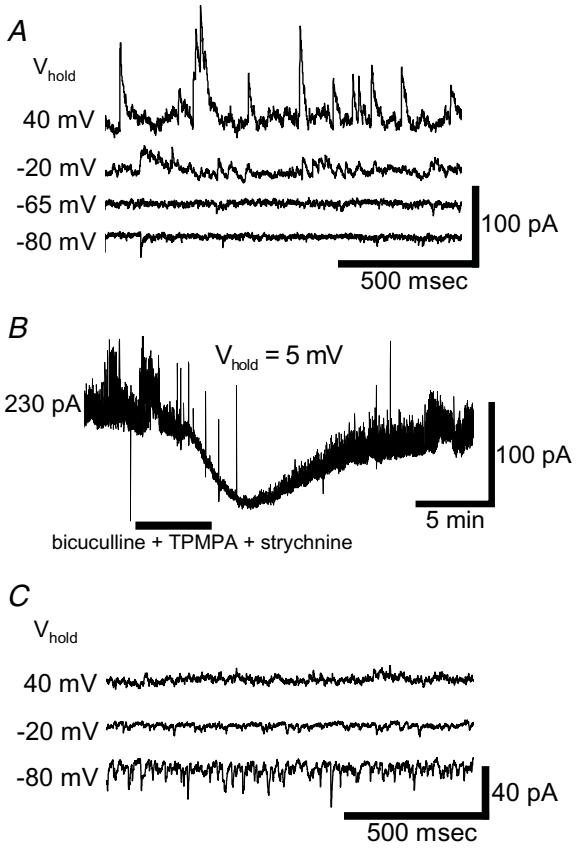

Figure 3. Inhibitory and excitatory synaptic inputs to ipRGCs are active at rest
A, voltage-clamp recordings of spontaneous synaptic currents of an ipRGC kept in darkness. Synaptic currents were inward at -80 mV, outward at -20 mV and $+40$ mV, and of minimal amplitude at -65 mV, suggesting they were mainly chloride-based and presumably mediated by ionotropic GABA and/or glycine receptors. Normal Ames' medium was in the bath. *B*, pharmacological analysis of spontaneous synaptic currents in another ipRGC. The cell was voltage clamped close to the cationic reversal potential to minimize glutamatergic currents. Blockade of ionotropic GABA and glycine receptors (30 μM (−)-bicuculline methochloride, 30 μM TPMPA and 5 μM strychnine) suppressed the synaptic events and decreased a basal outward current. *C*, spontaneous excitatory currents. In this ipRGC, amacrine cell inputs were continuously suppressed with the amacrine cell blocker cocktail (see Methods). Residual currents were inward at -80 mV and -20 mV but outward at $+40$ mV, indicating their cationic basis.

the continuous barrage of GABAergic and/or glycinergic synaptic inputs.

Glutamatergic synapses were also spontaneously active in darkness as indicated by the spontaneous synaptic events that occurred during continuous application of the amacrine cell cocktail, which antagonized GABA, glycine and cholinergic receptors. These synaptic events reversed near 0 mV ($n = 9$; Fig. 3*C*), suggesting that they are synaptic cationic conductances, presumably triggered by glutamatergic inputs from bipolar cells. Because the cationic synaptic currents could not be observed clearly unless the GABAergic and/or glycinergic transmission was blocked (compare Fig. 3*A* and *C*), inhibitory synaptic inputs appear to dominate in darkness under these recording conditions, at least as viewed from the soma.

All ipRGCs exhibit synaptically mediated light responses

Having confirmed that ipRGCs receive functional chemical synapses, we next asked whether these inputs were capable of generating light responses in these cells. We also wanted to understand how any such 'extrinsic' responses differed from melanopsin-based ('intrinsic') light responses and from the light-evoked responses of conventional RGCs. To address these questions, we were obliged to alter our method for targeting and recording ipRGCs, because the intense epi-illumination we used to visualize fluorescent retrograde labelling severely adapted the rods and cones and may even have irreversibly bleached them. Thus, we turned to the multielectrode array (MEA) recording technique in which ipRGCs can be identified from among the large number of simultaneously recorded ganglion cells on the basis of functional criteria alone, with no need for fluorescence imaging (Tu *et al.* 2005). An additional advantage of the MEA is that, as an extracellular recording method, it avoids the intracellular dialysis that occurs with the whole-cell method, which could affect synaptic responses.

A typical MEA recording of an ipRGC appears in Fig. 4. The cell's identity as an ipRGC was evident from the persistence of a robust, sustained light response when rod/cone signalling was blocked, from the long onset latency of this response, and from the prolonged post-stimulus discharge (Fig. 4, right). When synaptic blockers were omitted from the bathing solution (Fig. 4, left), the most dramatic difference was in the emergence of light responses to dim stimuli. Spikes were evoked by stimuli as much as six orders of magnitude dimmer than required to elicit firing through intrinsic phototransduction. This synaptically mediated response was generally very tonic, although near threshold it was relatively transient (Fig. 4 left, -6 and $-5 \log I$). In addition, the synaptically mediated light response had distinctive kinetics. Whereas the intrinsically mediated response was very sluggish at the intensities tested (e.g. latency of 5.4 s for the $+0.65 \log I$ response; Fig. 4 right), the synaptically mediated response was brisk at all stimulus intensities (e.g. latency of 0.06 s for the $+0.65 \log I$ response; Fig. 4 left). Moreover, at -6 to $-2 \log I$, the extrinsic response lacked the prominent poststimulus discharge of the intrinsic response. (The after-discharge at $-1 \log I$ in the control condition is not apparent in the presence of the rod/cone signalling blockers, suggesting a slight reduction in sensitivity for the intrinsic photoresponse in the drugs. This phenomenon was observed in most ipRGCs tested and was probably due to light adaptation, general rundown, and/or synaptic modulation of phototransduction gain; see the Discussion for more details.) Spontaneous activity also tended to

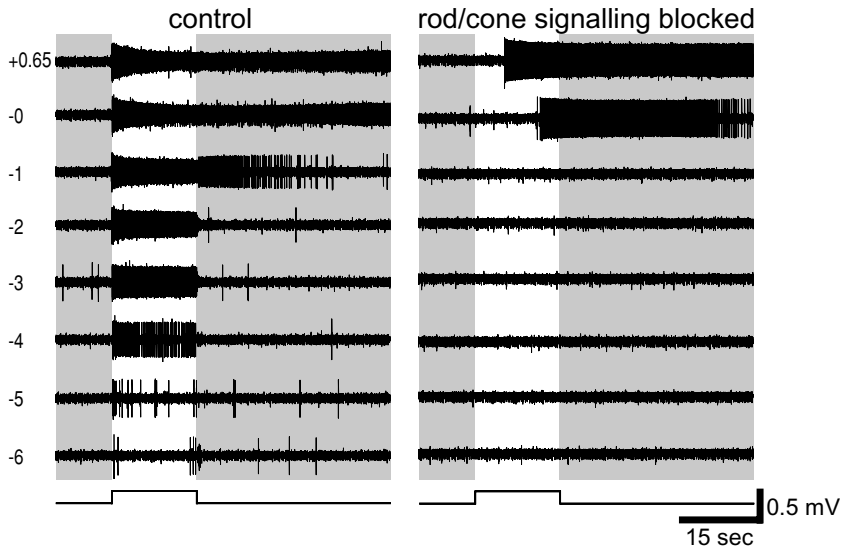

Figure 4. Multi-electrode array (MEA) recordings of synaptically mediated light responses in ipRGCs
Extracellular recordings comparing spike responses of an ipRGC to light of various intensities with rod/cone-driven synaptic inputs left intact (left) or blocked (right). Log stimulus attenuation is indicated to the left. Note that all responses to weaker stimuli (-2 log attenuation and dimmer) and short-latency responses to brighter ones (-1 to $+0.65$ log *I*) were dependent on synaptic transmission, presumably because they reflect rod and/or cone influence on the recorded cell. Note also that intensities sufficient to recruit the intrinsic response (-0 and $+0.65$ log *I*; right) evoke responses with substantial poststimulus persistence, a well-established feature of melanopsin-dependent light responses.

be slightly higher when synaptic circuits were functional than when they were blocked. There is some variation in spike amplitude in the responses to the brighter light stimuli; such variation is also seen routinely in whole-cell recordings (Fig. 6*A*; see also Wong *et al.* 2005*b*). In both types of recordings, attenuation in spike amplitude is associated with strong activation and is thus presumably caused by inactivation of voltage-gated sodium channels, that is, depolarization block.

All ipRGCs recorded by this method exhibited the features of the extrinsic light responses evident in Fig. 4 ($n = 82$). In every case, the synaptically driven light response consisted of an increase in spike rate that was relatively transient at threshold but more sustained when evoked by brighter light (Fig. 5*C*, left). The extrinsic responses were also consistently 4–6 orders of magnitude more sensitive than the pharmacologically isolated intrinsic ones (mean thresholds: -5.56 ± 0.13 and $-0.15 \pm 0.09 \log I$, respectively). In addition, the latency of the extrinsic light response was always significantly shorter than that of the pharmacologically isolated melanopsin light response. Measured at $+0.65 \log I$, the range of response latency of the extrinsic response was 0.05–0.06 s, while that of the intrinsic response was 0.4–14.9 s.

Thresholds for synaptically driven light responses were similar in conventional RGCs and ipRGCs, but such responses were consistently more sustained in ipRGCs. Figure 5*A* and *B* illustrates an example of this difference through simultaneous recording of a conventional RGC, which generated large-amplitude spikes, and an ipRGC, which emitted smaller action potentials. That only the latter unit was an ipRGC was evident from the persistence of its light response upon application of the rod/cone signalling blockers, whereas the large-amplitude unit was silenced (Fig. 5*A*, right). The ipRGC's light response in

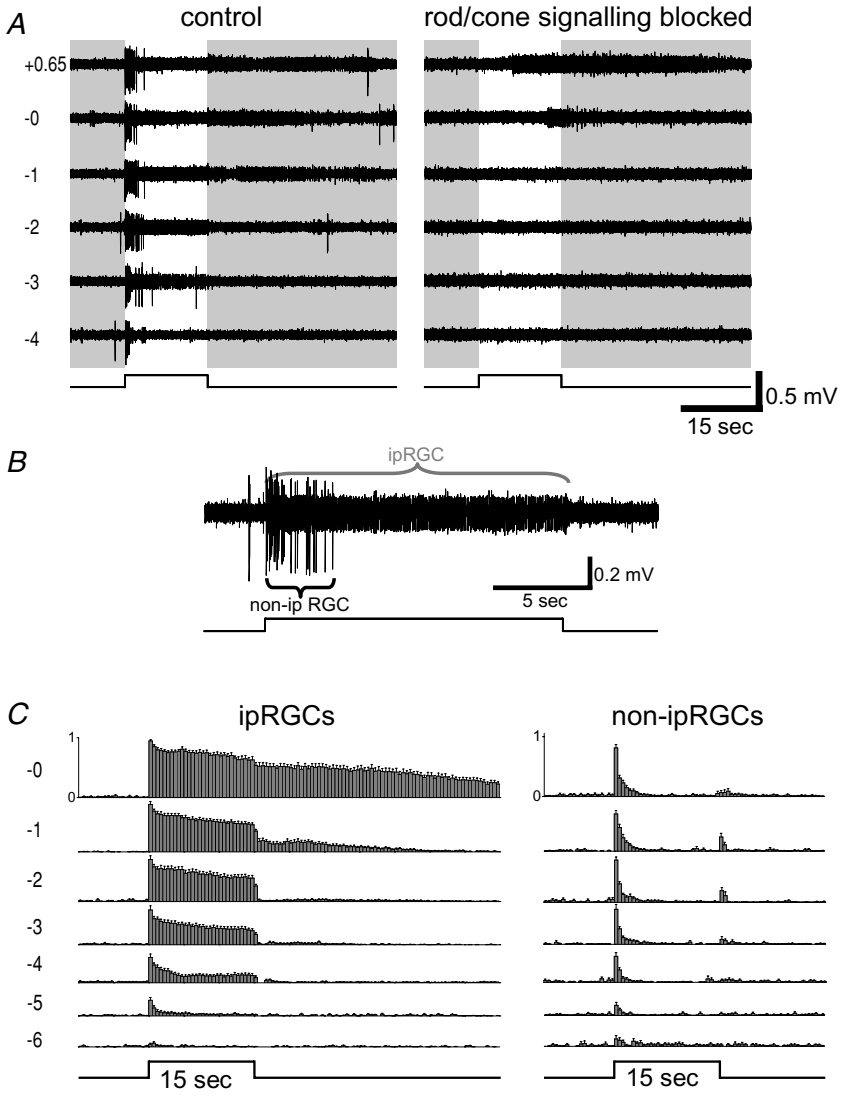

Figure 5. Differing kinetics of synaptically driven light responses in conventional and intrinsically photosensitive RGCs
A, simultaneous extracellular recordings from two different cells from a single electrode of the MEA. The larger spikes come from a conventional RGC and the smaller spikes from an ipRGC. The conventional RGC's light-evoked responses were transient at all stimulus intensities in normal Ames' medium (left), and were completely abolished in the presence of the rod/cone signalling blocker cocktail (right; see Methods). The ipRGC's responses were sustained in control medium even at light intensities too dim to evoke the intrinsic, melanopsin-based response (compare -3 and -2 log I traces, left and right). *B*, a magnified version of the '-2' response trace shown in *A*, left. The extrinsic light response of the ipRGC was more sustained than the light response of the conventional RGC, lasting throughout the duration of the light stimulus. *C*, a summary of the results from 12 ipRGCs (left) and 18 conventional RGCs (right). Action potentials from each trial were summed and plotted as a histogram with 0.5 s bins, and the largest-amplitude column from each cell was normalized to 1 (y axis in the '-0' response traces). These histograms were averaged to generate the histograms shown. The error bars represent S.E.M. values.

normal Ames' medium was sustained at every intensity except the weakest suprathreshold one (i.e. $-4 \log I$), even when the stimulus was too dim to activate the intrinsic photoresponse (Fig. 5*A* left, '−3' and '−2', and Fig. 5*B*). By contrast, in normal Ames' medium (Fig. 5*A*, left), the conventional RGC generated transient ON responses lasting no more than 4 s at any stimulus intensity. Similar behaviour was evident in nearly all conventional ON and ON–OFF RGCs tested ($n = \sim 40$), with the responses returning to baseline firing rates within 6 s during prolonged light steps. Such a difference in response kinetics between ipRGCs and conventional RGCs is summarized in Fig. 5*C*.

Amacrine cells and ON and OFF bipolar cells trigger light responses in ipRGCs

Synaptically driven light responses could also be detected in whole-cell recordings. The advantage of this approach over the MEA is that subthreshold voltage responses and reversal potentials can be measured. We therefore used such recordings in combination with pharmacology to determine which types of presynaptic cells mediate extrinsic light responses of ipRGCs.

Of the 74 ipRGCs recorded in the whole-cell configuration, 66 (89%) cells' light responses to a full-field, subsaturating pulse of white light consisted of an extrinsic component in addition to the intrinsic, melanopsin-based photoresponse. The remaining 11% failed to show any extrinsic light responses. Because extrinsic responses were evident in every ipRGC recorded by the MEA method, we suspect that their absence in these whole-cell recordings is a technical artefact. As noted above, for the whole-cell approach, bright illumination must be used to detect the fluorescent retrolabelling so that presumptive ipRGCs may be targeted for recording. The resulting bleaching of rods and cones can be expected to weaken their influence on ipRGCs or, in extreme cases, to eliminate them altogether. Indeed, even when extrinsic light responses were observed in the whole-cell studies, they were far less sensitive than those recorded using the MEA. In fact, their thresholds were similar to that of the endogenous melanopsin-driven response ($n > 20$; not shown), so that stimuli intense enough to evoke extrinsic light responses usually also induced the endogenous light response. Another difference between the two recording methods was that the ipRGC extrinsic light responses obtained in the whole-cell mode were much more transient than seen in the MEA. Figure 6*A* compares the light responses of a single ipRGC recording in control Ames' medium (left) and in the presence of synaptic blockers (right). The most obvious synaptically mediated component of the light response was a small transient depolarization and brief burst of spikes immediately after stimulus onset (Fig. 6*A*, left; arrow). The slow depolarization at onset and the persistent poststimulus depolarization evident in the same trace persisted in synaptic blockade (Fig. 6*A*, right) and are thus attributable to intrinsic melanopsin-based phototransduction. Both extrinsic (arrow) and intrinsic response components were also apparent under voltage clamp (Fig. 6*B*). We speculate that such transient responses were driven primarily by cone photoreceptors, because (1)

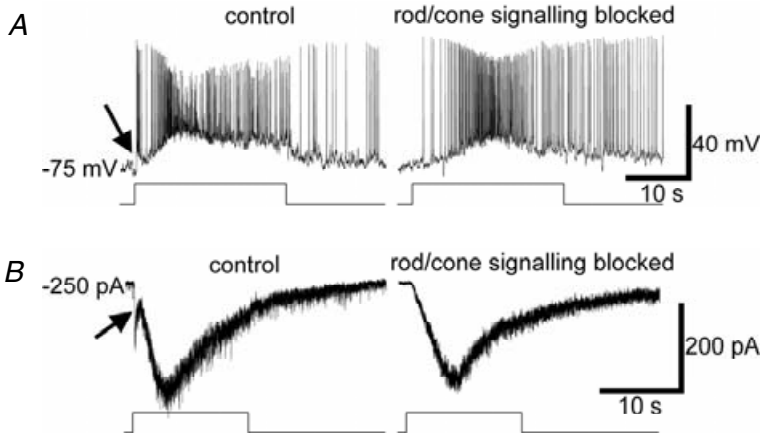

Figure 6. Whole-cell recordings of synaptically mediated light responses in ipRGCs
A, in current-clamp recordings, the response of this ipRGC to prolonged light stimuli consisted of a transient, relatively weak depolarizing synaptic response (arrow) followed by a slower and larger depolarization that outlasted the stimulus (left). The transient response was synaptically mediated (extrinsic), because it was selectively abolished by superfusion with the rod/cone signalling blocker cocktail (right), whereas the larger, slower depolarization and poststimulus response were melanopsin based because they survived the synaptic blockade. Stimulus intensity $= -3 \log I$. *B*, voltage-clamp recordings ($V_{hold} = -70$ mV) reveal the same two response components and confirm that the early, transient response (arrow) was selectively abolished by the rod/cone signalling blocker cocktail. Stimulus intensity $= -1 \log I$.

rod-driven responses would be much more sensitive than the intrinsic ipRGC response; (2) cone photoresponses are more transient than rod photoresponses; and (3) cone visual pigments are more resistant to bleaching than rhodopsin (Trevino *et al*. 2005). The more sustained and sensitive extrinsic light responses in the MEA recordings (see above) were probably generated mainly by rod photoreceptors.

To learn whether the extrinsic light responses of ipRGCs are mediated by amacrine cells, bipolar cells or both, we measured extrinsic light responses at various holding potentials under whole-cell voltage clamp. In normal Ames' medium, these responses occurred at light onset and consisted of conductance increases reversing at -57 ± 2 mV, close to the E_{rev} for chloride ($n = 6$; Fig. 7). This implies that under these recording conditions, amacrine-cell inputs gating ionotropic inhibitory conductances dominate the synaptically mediated light responses of ipRGCs.

However, bipolar cells can also drive light responses in ipRGCs. During continuous incubation in the amacrine blocker cocktail (see Methods), nearly all ipRGCs still generated extrinsic responses at light ON (14 of 15 cells; 93%). These consisted of conductance increases reversing at -4.0 ± 3.3 mV ($n = 5$; Fig. 8*A*), suggesting a non-specific cationic basis. In addition, the amacrine-cell blockade revealed an OFF response in most cells (10 of 14; 71%), consisting of an inward current (reversing at -3.3 ± 3.7 mV) or depolarization when the light pulse was extinguished (Fig. 8*A*). Such OFF responses were almost never observed in control medium, and were invariably smaller than the ON responses (arrows in Fig. 8*A*, left and Fig. 8*B*, left; compare with Figs 6*A* and *B*, left and Fig. 7, left). A parsimonious interpretation of these results is that the ON and OFF responses reflect light-driven glutamatergic inputs from ON and OFF bipolar cells, respectively, and that these inputs become more prominent when presynaptic and/or postsynaptic inhibition are relieved by amacrine-cell blockade. Consistent with this hypothesis, further addition of a selective blocker of the ON-bipolar-cell light response (L-AP4, a group III metabotropic glutamate receptor agonist; Slaughter & Miller, 1981) selectively abolished the ON depolarization while enhancing the OFF depolarization ($n = 8$; Fig. 8*B*, right). It also revealed an ON hyperpolarization. This was presumably caused by light-induced reduction of glutamate release from OFF bipolar cells onto ipRGCs, because most fast inhibition was blocked. In conclusion, amacrine cells, ON bipolar cells and OFF bipolar cells synapse directly onto ipRGCs, and at least under these recording conditions, amacrine cells provide the dominant synaptic input both spontaneously (Fig. 3) and in response to light stimulation. Light can nonetheless evoke depolarization and spiking, presumably because at the resting potentials (~ -60 to ~ -75 mV), driving force is stronger for cationic than for chloride conductances.

We also examined the basis of synaptic drive to ipRGCs using the MEA method, since it appears less vulnerable to distortions of response sensitivity and kinetics than the whole-cell recording method. Because MEA recordings are obtained extracellularly, we could not measure reversal potentials and instead relied on pharmacological manipulations to determine the presynaptic inputs that evoke extrinsic light responses in ipRGCs. First, we sought to confirm that bipolar cells contribute to the ipRGC extrinsic light response by documenting their persistence in the presence of amacrine-cell blockers (with TTX omitted, to permit the generation of sodium spikes). A typical result is shown in Fig. 9. To limit the evoked responses to those mediated synaptically, and also to minimize bleaching of rods and cones, only relatively dim stimulus light intensities (up to $-3 \log I$ in this example) were tested. In normal Ames' medium (left), this cell gave a relatively weak and transient response at -5 log I, typical of near-threshold responses recorded in

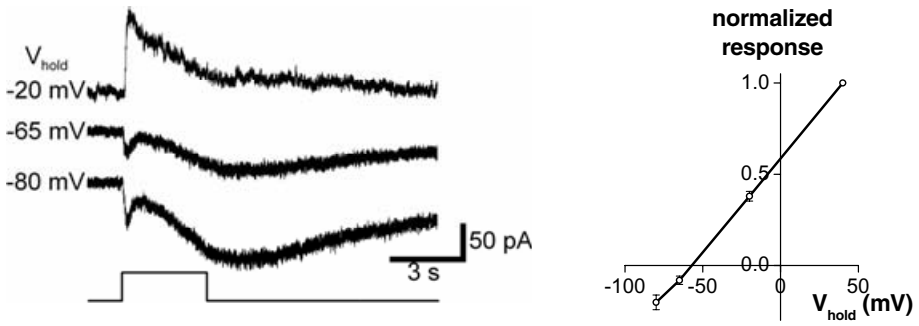

Figure 7. Light-induced synaptic inputs are mediated mainly by amacrine cells
In normal Ames' medium, the extrinsic light response (fast transient component at light onset) consisted of a conductance increase that reversed at around −60 mV, close to the calculated Nernst potential for chloride (see Methods). Left, current recordings at several holding potentials. Each trace is an average of several trials. Stimulus intensity = −2 log *I*. Right, baseline-subtracted *I–V* plot of peak transient light-evoked currents averaged from all six cells tested, with each cell's response amplitude at 40 mV normalized to 1. Error bars indicate S.E.M. values.

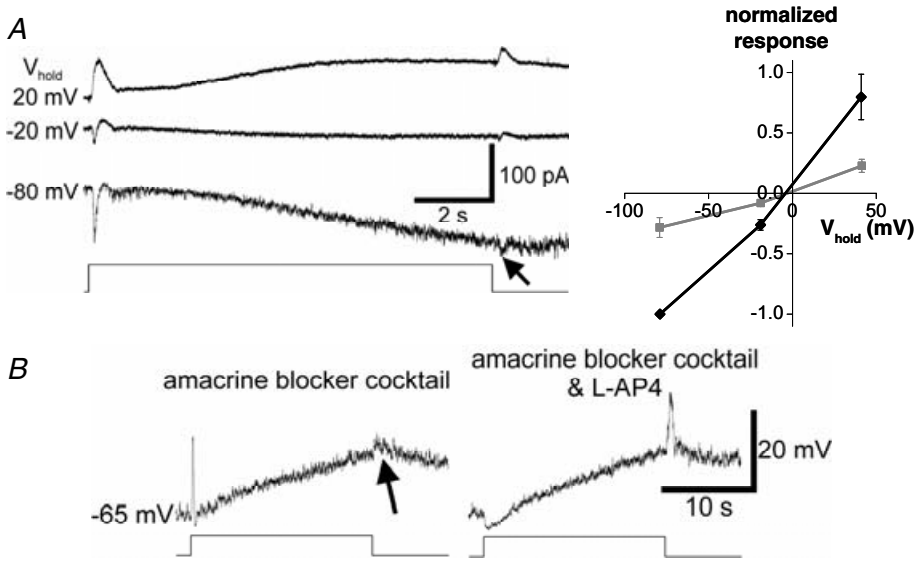

Figure 8. Light-induced synaptic inputs are also driven by ON and OFF bipolar cells
A, in the presence of pharmacological blockade of amacrine cell inputs (see Methods), the extrinsic light response reversed near 0 mV, implicating a cationic current. Left, current recordings at several holding potentials; the traces are averages of several responses. Note the small response at light OFF (arrow) in addition to the larger ON response. Light intensity = −2 log *I*. Right, baseline-subtracted *I–V* plot of peak currents evoked at light ON (black) and light OFF (grey), showing that these currents reversed near 0 mV and thus were mediated by an increase in cationic conductance. This plot was averaged from all five cells tested, with each cell's ON response amplitude at −80 mV normalized to −1. Error bars indicate S.E.M. values. *B*, voltage responses of another ipRGC in the same amacrine blocker cocktail similarly revealed components at light OFF (arrow) as well as at ON. The ON depolarization was selectively abolished by further addition of L-AP4 while the OFF response was enhanced, indicating that the OFF depolarization was generated by OFF bipolar cells rather than by the surround response of ON bipolar cells. Light intensity = −2.5 log *I*.

the MEA (see above). When the amacrine blocker cocktail was added to the bath (Fig. 9, right), two effects were noted. First, the ipRGC became spontaneously active in the dark. More importantly, the extrinsic light response not only survived the treatment but actually became stronger, resulting in a sustained response at −5 log *I* and pronounced depolarization block at higher light intensities (i.e. −4 and −3 log *I*). Similar results were obtained in all ipRGCs tested ($n = 18$). This result confirms that bipolar cells can drive sustained extrinsic light responses in ipRGCs. These effects of the cocktail also suggest that presynaptic and/or postsynaptic amacrine cell inputs

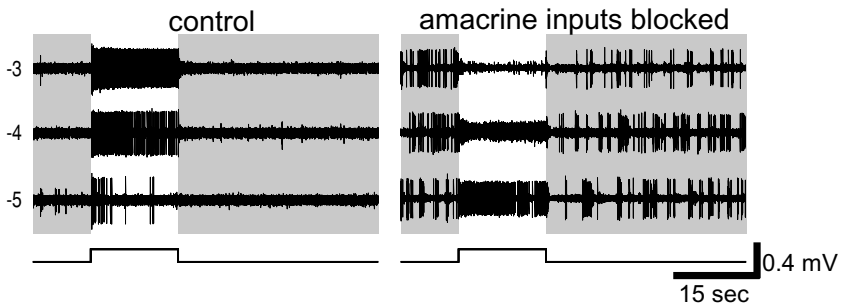

Figure 9. Bipolar cells can directly evoke sustained extrinsic light responses in ipRGCs
Voltage responses of a single well-isolated ipRGC, recorded extracellularly with an MEA electrode, to a series of light intensities all of which were subthreshold for intrinsic phototransduction. In the presence of the amacrine blocker cocktail with TTX omitted (right), the extrinsic light response of this ipRGC was sustained, just as it was in control Ames' medium (left, '−4' and '−3'). Under amacrine blockade, the extrinsic response became more robust and the responses to the −4 and −3 log *I* light flashes were so strong that depolarization block became evident. Amacrine blockade also increased the frequency of spontaneous spikes. Under both conditions, −6 log *I* light flashes did not evoke any response (not shown).

inhibit both spontaneous and light-evoked excitatory bipolar cell inputs to ipRGCs, thus preventing ipRGCs from spiking spontaneously and their light responses from inducing depolarization block.

In a second MEA experiment, we sought to confirm, under more physiological conditions, that the ON channel provides most of the input to generate the ipRGC extrinsic light response. Representative data are shown in Fig. 10*A*. Again, only relatively dim stimulus light intensities were tested to avoid activation of the intrinsic photoresponse and to minimize bleaching of rods and cones. Blocking the ON channel with L-AP4 abolished completely the increase in spiking during the light pulse for every cell tested ($n = 10$). In addition, for 7 of these 10 cells, ON-channel blockade induced a brief OFF response that was absent in control medium (Fig. 10*A* right, $-2 \log I$, and Fig. 10*B*). This effect of L-AP4 has been reported for non-ipRGCs (e.g. Arkin & Miller, 1988) and is consistent with the enhancement by L-AP4 of the OFF depolarization in whole-cell current-clamp recordings (Fig. 8*B*). A likely explanation is that in the absence of ON-channel blockade, withdrawal of ON-bipolar-cell input at light OFF results in disfacilitation, which counterbalances and masks the excitation from the OFF channel; silencing the ON channel unmasks the OFF channel input. In conclusion, while the ipRGC extrinsic light response is driven predominantly by the ON channel, the OFF channel (presumably through direct inputs from OFF bipolar cells) also makes a small contribution.

Mapping of the receptive field of the synaptically driven light response

To gain some insight into the anatomical distribution of the synaptic input to ipRGCs, we plotted receptive fields for the extrinsic light response (see Methods and Fig. 1*A*). A total of 15 ipRGCs were analysed using light spots that were subthreshold for the intrinsic response. The evoked responses, consisting of increases in firing during the presentation of the spot, appeared to be generated primarily in the ON channel, because virtually all of these responses were abolished in the presence of 100 μM L-AP4 ($n = 4$; not shown). All receptive fields had an oval shape similar to the example shown in Fig. 11*A*, with an average equivalent diameter of 957 ± 62 μm. For comparison, the receptive field of the melanopsin-based photoresponse was also mapped after eliminating extrinsic responses with the rod/cone signalling blockers (see Methods). The activation of intrinsic responses requires substantial spatial summation. We therefore replaced the mapping spot with an elongated bar stimulus. Also, because prolonged illumination is required to evoke an intrinsic response and because long interstimulus intervals are needed for recovery, we opted for a one-dimensional mapping protocol to limit the total time needed for mapping (see Methods and Fig. 1*B*). We analysed the melanopsin-based receptive fields of 18 ipRGCs, and the average width of these receptive fields was 820 ± 114 μm (Fig. 11*B*), which is not significantly different from the average diameter of

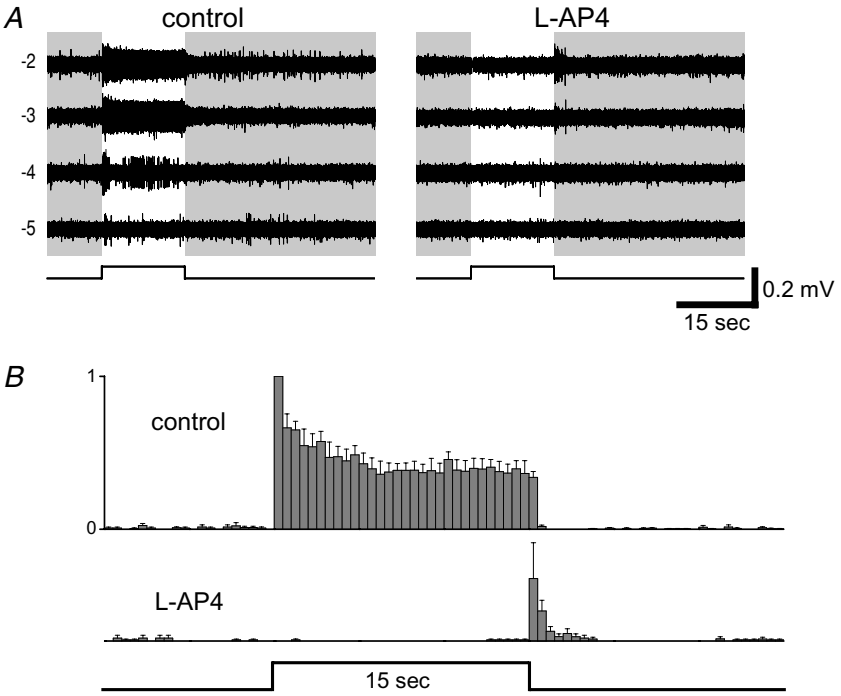

Figure 10. The ipRGC extrinsic light response is generated primarily by the ON channel
Effects of ON-channel blockade on extrinsic light responses of a single well-isolated ipRGC recorded extracellularly on the MEA. *A*, when 100 μM L-AP4 was applied to selectively block ON-bipolar-cell light responses and thus the rest of the ON channel, the extrinsic light response of this ipRGC was nearly completely abolished, and a few spikes were evoked at light offset (right). Notice that besides the larger spikes from the ipRGC, smaller spikes, presumably from other RGCs, were evoked at light offset in the presence of L-AP4 (seen most clearly in the -3 log *I* trace in the right column). *B*, a summary of the results from eight ipRGCs for the -2 log *I* responses, in control Ames' medium (top) and in 100 μM L-AP4 (bottom). Spikes from each trial were summed and plotted as a histogram with 0.5 s bins, and the largest-amplitude column from each cell was normalized to 1 (*y* axis in the 'control' response trace). These histograms were averaged to generate the histograms shown. The error bars indicate S.E.M. values.

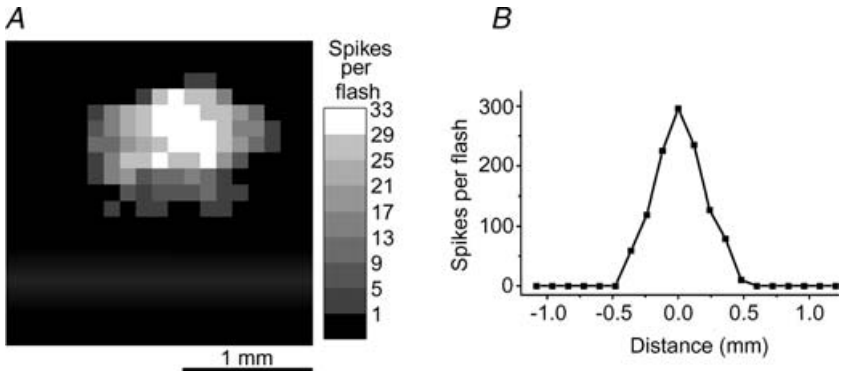

Figure 11. The receptive fields of extrinsic and intrinsic ipRGC responses
The receptive fields of the extrinsic and the intrinsic light responses have similar widths. *A*, the two-dimensional receptive field of the synaptically mediated light response of an ipRGC. Grey levels represent response amplitudes, in terms of the number of spikes induced by a 0.5 s white spot presented at that location (see Methods for detail). *B*, a one-dimensional receptive field plot of the melanopsin-driven intrinsic light response of another ipRGC. The *y* axis shows the number of spikes induced by a 19 s presentation of a white bar at the location indicated on the *x* axis.

the extrinsically generated receptive fields (Fig. 11*A*). Both measurements are substantially higher than the average dendritic field diameter of ipRGCs (∼500 μm; Berson *et al.* 2002). Because the resolution in both types of mapping experiments was 120 μm, the true values could have been overestimated by as much as 240 μm. In addition, some light scatter could have led to additional overestimation. The main point, however, is that the spatial extent of the excitatory synaptic input onto ipRGCs is comparable to that of the intrinsic light response, thus suggesting that ON bipolar cells make synaptic contacts onto the entire dendritic field of the ipRGCs.

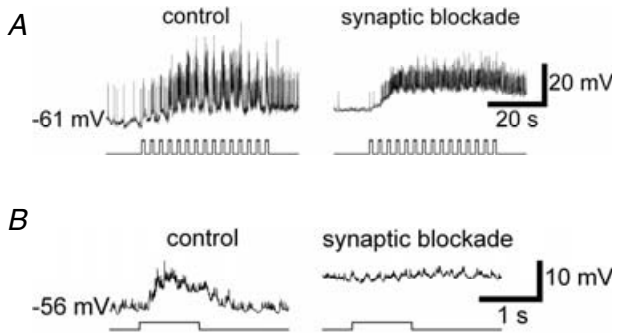

Figure 12. Synaptic inputs allow ipRGCs to respond to rapid fluctuations in light intensity
Flickering light (1 s duration, 0.33 Hz) evoked strongly modulated voltage responses in normal Ames' medium (*A*, left), but not under synaptic blockade (*A*, right; 40 μM DNQX, 60 μM D-AP5, 30 μM (−)-bicuculline methochloride, 30 μM TPMPA, and 5 μM strychnine). A sluggish unmodulated depolarization persisted under the cocktail, presumably reflecting temporal integration by the melanopsin system. Both response traces are averages of three trials. *B*, same as above, but showing averaged responses to one of the 1 s light pulses at higher temporal resolution (average of 45 responses, including all responses triggered by the three 40 s trains of flashes). Stimulus intensity = $-2 \log I$.

Influence of synaptic inputs on temporal bandpass

The preceding experiments showed that a major effect of synaptic inputs on ipRGCs is an increase in the sensitivity of these cells to light. Because the extrinsic response of an ipRGC to a single light pulse is faster than its melanopsin response, we suspected that synaptic input would also improve the ability of ipRGCs to encode modulations of light intensity at relatively high temporal frequencies. To test this idea, we examined the effects of synaptic blockade on the whole-cell response to a flickering stimulus. In control medium, the flicker (1 s square-wave pulses at 0.33 Hz) evoked two response components: small and fast depolarizing events that were time-locked to the individual light pulses; and an underlying, slowly developing depolarization that outlasted the train of light pulses (Fig. 12*A* and *B*, left). The modulation at the stimulus frequency was synaptically mediated because it was effectively abolished by the application of synaptic blockers, leaving only a sluggish unmodulated depolarization generated by the endogenous melanopsin mechanism (Fig. 12*A* and *B*, right). A similar result was observed in all cells tested ($n = 5$).

Discussion

We have obtained functional evidence that all ganglion-cell photoreceptors receive direct excitatory (presumably glutamatergic) synaptic input from bipolar cells and inhibitory input from GABAergic and/or glycinergic amacrine cells. Both the excitatory and inhibitory synapses are active at rest and stimulated by light. Most ipRGCs receive excitatory input from both ON and OFF bipolar cells, though the ON-bipolar inputs are substantially stronger. The ON-bipolar-cell-mediated receptive field covers the entire dendritic field of the ipRGCs. The

synaptically generated light responses of ipRGCs appear far more tonic than the light responses of conventional RGCs. In addition, the extrinsic light responses of ipRGCs are much more sensitive and faster than the melanopsin-based photoresponse, thus enabling these cells to respond to dimmer and faster-changing light stimuli than are detectable by the endogenous phototransduction.

A recent study by Perez-Leon *et al.* (2006) also reported the presence of both excitatory and inhibitory receptors in rat ipRGCs. Interestingly, the authors detected endogenous activation of glutamate and GABA receptors but not of glycine receptors, whereas all of our ipRGCs responded robustly to exogenously applied glycine, suggesting that the glycine receptors on ipRGCs are extrasynaptic. Future studies will be required to examine the functional roles of these receptors. In addition, Perez-Leon *et al.* (2006) found that only about 20% of all rat ipRGCs received any appreciable synaptic input, and that only a quarter of these exhibited synaptically mediated light responses. Two factors were probably responsible for the higher incidence of extrinsic light responses in our study. First, the intense epifluorescence illumination used in both studies to locate retrolabelling presumably resulted in less bleaching of rod and cone photopigments in our eyecup preparation, which retains the retinal pigment epithelium, than in the isolated retinas used by Perez-Leon *et al.* (2006). Second, our recordings were made at physiological temperature, whereas those in the other study were made at room temperature, which could cause the rod and cone photoreceptors to become significantly less light responsive (Mizota & Adachi-Usami, 2002).

Anatomical substrates of synaptic inputs to ipRGCs

The excitatory synaptic inputs to ipRGCs documented here presumably arise from bipolar cells, because the excitation is primarily or exclusively glutamatergic, and bipolar cells are the sole source of glutamatergic input to ganglion cells (but see Johnson *et al.* 2004). We attribute the synaptic inhibition of ipRGCs to direct contacts from GABAergic and/or glycinergic amacrine cells, as these are the only cell types known to be capable of triggering the observed chloride conductances.

Both ON and OFF bipolar cells apparently contact ipRGCs because both the onset and termination of a light pulse evoked cationic conductances, and because only the response at stimulus onset was abolished by a selective ON-channel blocker. However, the ON-bipolar input is much stronger. Our receptive field maps shed new light on the spatial arrangement of synaptic inputs onto the dendritic fields of the ipRGCs. Because the intrinsic response is generated throughout the somadendritic membrane, the receptive field of this response closely matches the dendritic field (Berson *et al.* 2002). We find that the receptive field for the synaptically mediated, depolarizing extrinsic response has similar spatial dimensions, suggesting that ipRGCs receive ON-bipolar inputs throughout their dendritic fields. This is surprising because ipRGC dendrites terminate mainly within the OFF sublayer of the IPL. Only a small fraction of the dendritic arbour of an ipRGC, mainly its proximal, lower-order branches, traverses the ON sublayer (Berson *et al.* 2002; Hattar *et al.* 2002; Provencio *et al.* 2002). If ON-bipolar synaptic contacts onto ipRGC were restricted to the ON sublayer, one would expect the extrinsic receptive fields of these cells to be smaller than the dendritic fields and the receptive field of the intrinsic response.

What accounts for the observed larger receptive fields? It is possible that ipRGCs are contacted by atypical ON bipolar cells that make at least a few synaptic contacts in the OFF sublayer in the outer IPL (Pang *et al*. 2004; Wong & Dowling, 2005). This seemingly implausible model receives support from the finding that displaced primate ipRGCs with somata in the inner nuclear layer, and dendrites entirely confined to the OFF sublayer, exhibit robust, synaptically driven ON depolarizing responses (Dacey *et al.* 2005). Furthermore, dopaminergic amacrine cells with processes stratifying only in the OFF sublayer have been shown to generate predominantly depolarizing light responses (Zhang *et al.* 2004, 2007). However, in an electron microscopic study of synaptic inputs to melanopsin-immunopositive dendrites in the mouse retina, Belenky *et al.* (2003) reported ribbon (bipolar-cell) contacts only in the proximal (ON) sublayer of the IPL; none were detected in the OFF sublayer. If bipolar inputs are similarly restricted to the ON sublayer in the rat, then the correspondence we observe between dendritic fields and synaptically mediated receptive fields of ipRGC seems to imply substantial spatial broadening in the rod/cone circuitry at a level presynaptic to the ipRGCs' dendrites. This might be achieved by bipolar cells with unusually large dendritic arbours in the outer plexiform layer or axonal terminal fields in the IPL, or by electrical coupling between bipolar cells. Coupling between ipRGCs seems an unlikely mechanism for broadening because this would presumably expand the receptive field of the intrinsic response as well. Further experiments will be needed to distinguish among these possibilities.

Amacrine cells also make functional synaptic contacts onto ipRGCs, because our whole-cell recordings in control medium revealed evoked synaptic currents at light onset that reversed near the chloride reversal potential. These inhibitory synaptic inputs are consistent with the conventional (amacrine-cell) synapses in the ON sublamina of the IPL reported by Belenky *et al.* (2003). The same study also found conventional synapses made onto melanopsin-immunopositive processes in the OFF sublayer, but we never observed chloride-mediated inhibitory synaptic responses at light offset. While this

could be an artefact of our eyecup preparation, it is also possible that the amacrine cell contacts in the OFF sublamina release onto ipRGCs' slow-acting neuromodulators (e.g. substance P, dopamine, etc) that do not directly trigger transmembrane voltage or current changes. Consistent with this possibility, Sakamoto *et al.* (2005) reported that ipRGCs express dopamine receptors and that D_2 receptor agonists can modulate melanopsin mRNA levels in ipRGCs. Further studies will be needed to investigate whether these dopamine receptors are present in the ipRGC dendrites in the OFF sublayer, and whether other neuromodulators can also influence ipRGCs.

A schematic summary of the synaptic circuits inferred from our findings appears in Fig. 13.

Response kinetics of extrinsic input to ipRGCs

In MEA recordings of ipRGCs, rod/cone-driven light responses were transient when evoked by near-threshold stimuli (e.g. -6 and $-5 \log I$ in Figs 4 and 5*C*), but became sustained at higher intensities (e.g. $-4 \log I$ in Figs 4 and 5*C*). The transient responses to dim light intensities could be due to the simultaneous activation of both centre and surround regions of the ipRGC receptive field by the full-field light stimuli used. However, by using centre-selective light stimuli, Dacey *et al.* (2005) found that near-threshold light stimuli likewise evoked rapidly adapting spiking responses in primate ipRGCs (see Fig. 3*C* in that study). The same study further reported a lack of antagonistic surround in the receptive field of the synaptically mediated ipRGC light response. Thus, the relatively transient extrinsic responses to dim light that we observed in rat ipRGCs probably reflect light adaptation of the rod photoreceptors.

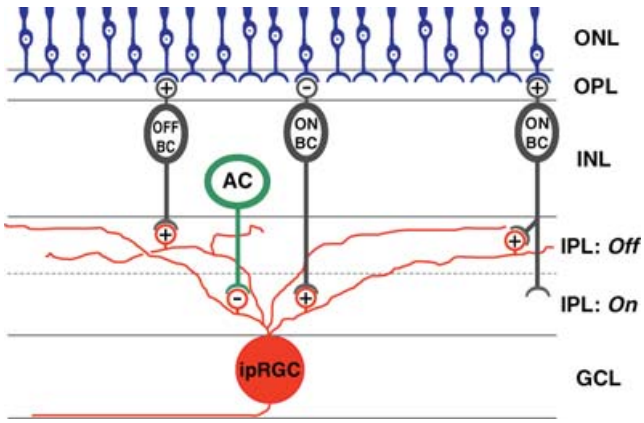

Figure 13. Summary diagram of synaptic inputs to ipRGCs
Schematic diagram summarizing the synaptic circuits inferred from results of the present study. Amacrine cells can evoke inhibitory light responses in ipRGCs at light onset, whereas ON and OFF bipolar cells can trigger excitatory light responses in ipRGCs at light onset and offset, respectively. Synaptic inputs from the ON bipolar cells appear to cover the entire ipRGC dendritic field, and thus might include both conventional ON bipolar cells contacting proximal dendrites of ipRGCs in the ON sublamina of the inner plexiform layer (middle bipolar) and atypical ON bipolar cells making synaptic contacts in the OFF sublamina (right bipolar). '+' and '−' symbols represent excitatory and inhibitory receptors, respectively. ONL, outer nuclear layer; OPL, outer plexiform layer; INL, inner nuclear layer; IPL, inner plexiform layer; GCL, ganglion cell layer; OFF BC, OFF bipolar cell; ON BC, ON bipolar cell; AC, amacrine cell; ipRGC, intrinsically photosensitive retinal ganglion cell.

The ability of ipRGCs to maintain robust synaptically mediated light responses to steady illumination appears to be a distinctive feature of this ganglion cell type, at least under our recording conditions, because the great majority of conventional RGCs stopped responding to constant light after a few seconds (Fig. 5). Very sustained synaptically mediated light responses have also been reported for primate ipRGCs (Dacey *et al.* 2005), for presumed cat ipRGCs (Pu, 2000), and for certain ganglion cells possibly corresponding to ipRGCs that have been described in classic studies of cat and rabbit retinas, variously termed 'luminance units', 'on sluggish sustained cells' or 'ON tonic W-cells' (Barlow & Levick, 1969; Cleland & Levick, 1974; Stone & Fukuda, 1974). This tonic drive from the outer retina is consonant with the unusually sustained quality of the direct, melanopsin-mediated photoresponse of ipRGCs (Berson *et al.* 2002; Dacey *et al.* 2005). In this sense, the synaptic circuits linking classical photoreceptors to ipRGCs may be specialized to extend the ability of ipRGCs to stably encode light intensity beyond the dynamic range offered by melanopsin phototransduction alone.

The functional basis of the unusually tonic rod/cone drive to these cells is unknown. One possibility is that ipRGCs draw synaptic contacts selectively from specific bipolar cell types that generate unusually sustained light responses. Indeed, ipRGC dendrites terminate within the outermost level of the IPL (Berson *et al.* 2002; Hattar *et al.* 2002; Provencio *et al.* 2002), and there is evidence that bipolar cells and RGCs that stratify in the margins of the IPL tend to generate relatively sustained light responses (Awatramani & Slaughter, 2000; Roska & Werblin, 2001). Alternatively, or additionally, bipolar axon terminals presynaptic to the ipRGCs may be less subject than other bipolar terminals to presynaptic inhibition from amacrine cells. Yet another possibility is that the intrinsic membrane properties of ipRGCs could be specialized to minimize spike accommodation and thus reflect in their spike trains the sustained component of their bipolar input (but see Warren *et al.* 2003).

A final possibility that should be considered is that the extrinsic inputs to ipRGCs inferred from the MEA data are really no more sustained that those to other RGCs, but are made to appear so by a covert contribution from the intrinsic phototransduction mechanism. Specifically, the slowly rising intrinsic depolarization triggered by

just-suprathreshold phototransduction (Berson *et al.* 2002) might compensate for progressive adaptation of the extrinsic response to produce a steady level of total depolarization. Though the available data do not exclude such a possibility, they make it unlikely. First, because conventional RGCs maintain almost no increase in spike frequency at the end of the 15 s light pulse (Fig. 5*C*, right), the maintained firing in ipRGCs would, according to this hypothesis, have to be supported almost entirely by intrinsic phototransduction. If this were true, given the slow shutoff kinetics of this response, one could expect to see at least some poststimulus discharge, but instead the discharge stops abruptly (e.g. Figure 5*C* left, -4 to $-2 \log I$). Second, whole-cell recordings show that the latency of the depolarizing melanopsin response exhibits a steep inverse relation to stimulus intensity. Reductions in stimulus intensity of less than 1 log unit can increase the latency of a detectable depolarization from several seconds to nearly a minute (Fig. 3 of Berson *et al.* 2002). It is unclear therefore how melanopsin-driven subthreshold depolarization can support sustained firing during the latter part of a 15 s stimulus over a range of 3 log units of intensity (Fig. 5*C* left, -4 to $-2 \log I$). More generally, the hypothesized mechanism would require almost perfectly complementary intensity dependence of the kinetics of the extrinsic and intrinsic responses at each light intensity, to produce the very stable spike rates observed. Any mismatch would produce a biphasic temporal profile in the post-stimulus time histograms, and this is not observed (Fig. 5*C* left, -4 to $-2 \log I$). Finally, whole-cell recordings of primate ipRGCs show that light intensities too dim to elicit any melanopsin-based graded potential change evoked remarkably sustained extrinsic light responses (Dacey *et al.* 2005).

We have attributed the transience of extrinsic light responses in whole-cell recordings, relative to the sustained responses in MEA, to compromised integrity of rod/cone function in the former, probably from bright epifluorescence illumination. However, another possibility should be considered. There is emerging evidence for the existence of a second type of melanopsin-expressing ganglion cell in rodent retina, with dendritic stratification in the proximal IPL (Provencio *et al.* 2002; Hattar *et al.* 2006; A. Castrucci, I. Provencio, and D. Berson, unpublished observations). It has yet to be demonstrated that these cells are intrinsically photosensitive, but Tu *et al.* (2005) have identified two functionally distinct populations of ipRGCs in MEA recordings that could conceivably correspond to the proximally and distally stratifying varieties of melanopsin RGCs. All of our whole-cell recordings were presumably made from the distally stratifying cells, because only these cells have been filled from the SCN and recorded (Berson *et al.* 2002). However, if the proximally stratifying population is intrinsically photosensitive and contributes to the sample of ipRGCs recorded by the MEA, the difference in kinetics between MEA and whole-cell recordings may be at least partly attributable to functional distinctions between the proximal and distal types. However, it seems very unlikely that the MEA method would exhibit such a strong sampling bias for the proximally stratifying type that none of the recorded ipRGCs would have been of the distally stratifying type. Because all ipRGCs recorded by the MEA had very tonic extrinsic inputs, this must be true of distally stratifying melanopsin-expressing cells.

Functional roles of extrinsic input to ipRGCs

The present findings indicate that all ipRGCs receive photically driven synaptic inputs. These cells, through their projections to specific brain nuclei, are thus a significant source of the rod and cone signals that are known to affect the non-image-forming visual systems of the brain. Rod and cone influence on the circadian system has been inferred from the photic responses of SCN neurons (Aggelopoulos & Meissl, 2000). It is also evident from the persistence of photic phase resetting in melanopsin knockout mice (Panda *et al.* 2002; Ruby *et al.* 2002), despite the loss of direct photosensitivity of ipRGCs in these animals (Lucas *et al.* 2003; Tu *et al.* 2005). The action spectrum for circadian phase resetting resembles that of rods or M cones in wild-type mice but matches the spectral behaviour of melanopsin in mice with defective rod and cone systems (Yoshimura & Ebihara, 1996; Hattar *et al.* 2003; Dkhissi-Benyahya *et al.* 2007). Evidence for convergence of signals from classical photoreceptors and melanopsin has also emerged from analysis of other non-image-forming visual functions. Though ipRGCs support a pupillary light reflex in the absence of rods and cones (Lucas *et al.* 2003), conventional photoreceptors dominate the action spectrum of the reflex in wild-type animals (Lucas *et al.* 2001; Gamlin *et al.* 2007) and are essential for pupillary responses when the light is dim (Lucas *et al.* 2003; Gamlin *et al.* 2007) or when melanopsin deletion has abolished the intrinsic photosensitivity of ipRGCs (Hattar *et al.* 2002, 2003). Similarly, the acute suppression of locomotor activity by light ('negative masking') can be triggered by activation of either classical photoreceptors or ipRGCs (Mrosovsky *et al.* 1999; Panda *et al.* 2002; Hattar *et al.* 2003; Mrosovsky & Hattar, 2003).

The ipRGCs are not the only potential source of rod and cone influence on these brain mechanisms. Conventional RGCs may innervate brain nuclei mediating non-image-forming visual functions either directly (Gooley *et al.* 2003; Morin *et al.* 2003; Hattar *et al.* 2006) or through polysynaptic pathways involving other retinorecipient nuclei such as the intergeniculate leaflet. However, preliminary behavioural data have shown that

selective transgenic ablation of ipRGCs in mice largely abolishes the pupillary light reflex, negative masking responses, and photic entrainment of circadian rhythms (J. Ecker, A. Guler, R.J. Lucas, & S. Hattar, *Association for Research in Vision & Ophthalmology*, 2007), suggesting that ipRGCs may be the main if not the only route through which rods and cones exert functional control over these non-image-forming visual behaviours.

A salient feature of the synaptically driven light responses in ipRGCs is that they are significantly more sensitive than the endogenous response. Thus, they permit ipRGCs to detect light stimuli far dimmer than those detectable by the melanopsin phototransduction mechanism. Indeed, the pupillary light reflex has been reported to be up to 4 log units more sensitive in wild-type mice than in mice lacking functional rods and cones (Lucas *et al.* 2001, 2003). Similarly, rod/cone signalling enables wild-type mice to display masking responses to light intensities several log units below the threshold for melanopsin photoresponses (Mrosovsky & Hattar, 2003). However, a long-standing conundrum is that even though circadian photoentrainment is driven partly by rod photoreceptors, its absolute sensitivity is considerably lower than that of rod vision (Takahashi *et al.* 1984). Our data may provide a partial explanation: rod/cone-driven light responses in ipRGCs were transient when evoked by the dimmest stimuli tested (presumably near the threshold for rod photoresponses) and became more sustained only at intensities that were about 2 log units higher (Fig. 5*C*, left). We speculate that sustained light-induced discharge may be required to trigger measurable circadian phase shifts.

Besides extending the dynamic range of ipRGCs in the intensity domain, synaptic inputs also extend the bandpass of ipRGCs in the temporal frequency domain. While the ability to generate rapid responses to light stimuli may be unnecessary for many non-image-forming visual behaviours such as circadian entrainment and modulation of melatonin release, it is important to other responses such as the pupillary light reflex, which can be activated within a few hundred milliseconds after light onset and has been shown to be delayed by several seconds after intraocular injection of glutamate analogues to block rod/cone signalling (Gamlin *et al.* 2007).

A potential third function of synaptic input is to modulate the endogenous photoresponse of ipRGCs through alteration of the membrane conductance, influx of calcium through voltage-gated calcium channels, and/or interactions of metabotropic receptor mechanisms with the phototransduction cascade. There is little compelling evidence for such effects in the data presented here. Although we typically found higher thresholds for the intrinsic photoresponse in synaptic blockade than in control medium in MEA experiments (Fig. 4), this effect could be easily attributed to the fact that the recordings in synaptic blockade were invariably made after those in control medium. As a result, the intrinsic light response recorded in synaptic blockade was in a more light-adapted state (Wong *et al.* 2005*b*) than that recorded in control medium, and the preparation may have undergone modest reductions in functional health, either of which could have lowered the sensitivity of the intrinsic response. Consistent with these possibilities, the threshold for the intrinsic photoresponse was usually elevated further after the synaptic blockers had been washed off (not shown). We have, however, found in preliminary whole-cell recording studies ($n = 8$ ipRGCs) that simultaneously blocking glutamate, GABA and glycine receptors with antagonists increased the amplitude of the melanopsin voltage response to subsaturating light by about 50% (not shown). Thus, one of the functions of synaptic inputs to ipRGCs might indeed be modulation of the melanopsin photoresponse, although such a conclusion needs to be confirmed under more physiological conditions, and its relevance (if any) to non-image-forming visual behaviours needs to be investigated.

References

Aggelopoulos NC & Meissl H (2000). Responses of neurones of the rat suprachiasmatic nucleus to retinal illumination under photopic and scotopic conditions. *J Physiol* **523**, 211–222.

Arkin MS & Miller RF (1988). Synaptic inputs and morphology of sustained ON-ganglion cells in the mudpuppy retina. *J Neurophysiol* **60**, 1143–1159.

Awatramani GB & Slaughter MM (2000). Origin of transient and sustained responses in ganglion cells of the retina. *J Neurosci* **20**, 7087–7095.

Barlow HB & Levick WR (1969). Changes in the maintained discharge with adaptation level in the cat retina. *J Physiol* **202**, 699–718.

Belenky MA, Smeraski CA, Provencio I, Sollars PJ & Pickard GE (2003). Melanopsin retinal ganglion cells receive bipolar and amacrine cell synapses. *J Comp Neurol* **460**, 380–393.

Berson DM, Dunn FA & Takao M (2002). Phototransduction by retinal ganglion cells that set the circadian clock. *Science* **295**, 1070–1073.

Cleland BG & Levick WR (1974). Brisk and sluggish concentrically organized ganglion cells in the cat's retina. *J Physiol* **240**, 421–456.

Dacey DM, Liao HW, Peterson BB, Robinson FR, Smith VC, Pokorny J, Yau KW & Gamlin PD (2005). Melanopsin-expressing ganglion cells in primate retina signal colour and irradiance and project to the LGN. *Nature* **433**, 749–754.

Dkhissi-Benyahya O, Gronfier C, De Vanssay W, Flamant F & Cooper HM (2007). Modeling the role of mid-wavelength cones in circadian responses to light. *Neuron* **53**, 677–687.

Dunn FA & Berson DM (2002). Are intrinsically photosensitive retinal ganglion cells influenced by rods or cones? *Association for Research in Vision and Ophthalmology* Abstract no. 2982.

Ecker J, Guler A, Lucas RJ, & Hattar S (2007). Genetic Ablation of melanopsin-Containing Retinal Ganglion Cells Severely Attenuates Light-Dependent Physiological Functions. *Association for Research in Vision and Ophthalmology* Abstract no. 2989.

Fu Y, Zhong H, Wang MH, Luo DG, Liao HW, Maeda H, Hattar S, Frishman LJ & Yau KW (2005). Intrinsically photosensitive retinal ganglion cells detect light with a vitamin A-based photopigment, melanopsin. *Proc Natl Acad Sci U S A* **102**, 10339–10344.

Gamlin PD, McDougal DH, Pokorny J, Smith VC, Yau KW & Dacey DM (2007). Human and macaque pupil responses driven by melanopsin-containing retinal ganglion cells. *Vision Res* **47**, 946–954.

Gooley JJ, Lu J, Chou TC, Scammell TE & Saper CB (2001). Melanopsin in cells of origin of the retinohypothalamic tract. *Nat Neurosci* **4**, 1165.

Gooley JJ, Lu J, Fischer D & Saper CB (2003). A broad role for melanopsin in nonvisual photoreception. *J Neurosci* **23**, 7093–7106.

Hannibal J & Fahrenkrug J (2002). Melanopsin: a novel photopigment involved in the photoentrainment of the brain's biological clock? *Ann Med* **34**, 401–407.

Hannibal J, Hindersson P, Knudsen SM, Georg B & Fahrenkrug J (2002). The photopigment melanopsin is exclusively present in pituitary adenylate cyclase-activating polypeptide-containing retinal ganglion cells of the retinohypothalamic tract. *J Neurosci* **22**, RC191.

Hattar S, Kumar M, Park A, Tong P, Tung J, Yau KW & Berson DM (2006). Central projections of melanopsin-expressing retinal ganglion cells in the mouse. *J Comp Neurol* **497**, 326–349.

Hattar S, Liao HW, Takao M, Berson DM & Yau KW (2002). Melanopsin-containing retinal ganglion cells: architecture, projections, and intrinsic photosensitivity. *Science* **295**, 1065–1070.

Hattar S, Lucas RJ, Mrosovsky N, Thompson S, Douglas RH, Hankins MW, Lem J, Biel M, Hofmann F, Foster RG & Yau KW (2003). Melanopsin and rod-cone photoreceptive systems account for all major accessory visual functions in mice. *Nature* **424**, 76–81.

Johnson J, Sherry DM, Liu X, Fremeau Rt Jr, Seal RP, Edwards RH & Copenhagen DR (2004). Vesicular glutamate transporter 3 expression identifies glutamatergic amacrine cells in the rodent retina. *J Comp Neurol* **477**, 386–398.

Lucas RJ, Douglas RH & Foster RG (2001). Characterization of an ocular photopigment capable of driving pupillary constriction in mice. *Nat Neurosci* **4**, 621–626.

Lucas RJ, Hattar S, Takao M, Berson DM, Foster RG & Yau KW (2003). Diminished pupillary light reflex at high irradiances in melanopsin-knockout mice. *Science* **299**, 245–247.

Melyan Z, Tarttelin EE, Bellingham J, Lucas RJ & Hankins MW (2005). Addition of human melanopsin renders mammalian cells photoresponsive. *Nature* **433**, 741–745.

Mizota A & Adachi-Usami E (2002). Effect of body temperature on electroretinogram of mice. *Invest Ophthalmol Vis Sci* **43**, 3754–3757.

Morin LP, Blanchard JH & Provencio I (2003). Retinal ganglion cell projections to the hamster suprachiasmatic nucleus, intergeniculate leaflet, and visual midbrain: bifurcation and melanopsin immunoreactivity. *J Comp Neurol* **465**, 401–416.

Mrosovsky N, Foster RG & Salmon PA (1999). Thresholds for masking responses to light in three strains of retinally degenerate mice. *J Comp Physiol [A]* **184**, 423–428.

Mrosovsky N & Hattar S (2003). Impaired masking responses to light in melanopsin-knockout mice. *Chronobiol Int* **20**, 989–999.

Newman LA, Walker MT, Brown RL, Cronin TW & Robinson PR (2003). Melanopsin forms a functional short-wavelength photopigment. *Biochemistry* **42**, 12734–12738.

Panda S, Nayak SK, Campo B, Walker JR, Hogenesch JB & Jegla T (2005). Illumination of the melanopsin signalling pathway. *Science* **307**, 600–604.

Panda S, Provencio I, Tu DC, Pires SS, Rollag MD, Castrucci AM, Pletcher MT, Sato TK, Wiltshire T, Andahazy M, Kay SA, Van Gelder RN & Hogenesch JB (2003). Melanopsin is required for non-image-forming photic responses in blind mice. *Science* **301**, 525–527.

Panda S, Sato TK, Castrucci AM, Rollag MD, Degrip WJ, Hogenesch JB, Provencio I & Kay SA (2002). Melanopsin (Opn4) requirement for normal light-induced circadian phase shifting. *Science* **298**, 2213–2216.

Pang JJ, Gao F & Wu SM (2004). Stratum-by-stratum projection of light response attributes by retinal bipolar cells of Ambystoma. *J Physiol* **558**, 249–262.

Perez-Leon JA, Warren EJ, Allen CN, Robinson DW & Brown RL (2006). Synaptic inputs to retinal ganglion cells that set the circadian clock. *Eur J Neurosci* **24**, 1117–1123.

Provencio I, Jiang G, De Grip WJ, Hayes WP & Rollag MD (1998). Melanopsin: An opsin in melanophores, brain, and eye. *Proc Natl Acad Sci U S A* **95**, 340–345.

Provencio I, Rollag MD & Castrucci AM (2002). Photoreceptive net in the mammalian retina. This mesh of cells may explain how some blind mice can still tell day from night. *Nature* **415**, 493.

Pu M (2000). Physiological response properties of cat retinal ganglion cells projecting to suprachiasmatic nucleus. *J Biol Rhythms* **15**, 31–36.

Qiu X, Kumbalasiri T, Carlson SM, Wong KY, Krishna V, Provencio I & Berson DM (2005). Induction of photosensitivity by heterologous expression of melanopsin. *Nature* **433**, 745–749.

Rollag MD, Berson DM & Provencio I (2003). Melanopsin, ganglion-cell photoreceptors, and mammalian photoentrainment. *J Biol Rhythms* **18**, 227–234.

Roska B & Werblin F (2001). Vertical interactions across ten parallel, stacked representations in the mammalian retina. *Nature* **410**, 583–587.

Ruby NF, Brennan TJ, Xie X, Cao V, Franken P, Heller HC & O'Hara BF (2002). Role of melanopsin in circadian responses to light. *Science* **298**, 2211–2213.

Sakamoto K, Liu C, Kasamatsu M, Pozdeyev NV, Iuvone PM & Tosini G (2005). Dopamine regulates melanopsin mRNA expression in intrinsically photosensitive retinal ganglion cells. *Eur J Neurosci* **22**, 3129–3136.

Sekaran S, Foster RG, Lucas RJ & Hankins MW (2003). Calcium imaging reveals a network of intrinsically light-sensitive inner-retinal neurons. *Curr Biol* **13**, 1290–1298.

Semo M, Peirson S, Lupi D, Lucas RJ, Jeffery G & Foster RG (2003). Melanopsin retinal ganglion cells and the maintenance of circadian and pupillary responses to light in aged rodless/coneless (rd/rd cl) mice. *Eur J Neurosci* **17**, 1793–1801.

Slaughter MM & Miller RF (1981). 2-amino-4-phosphonobutyric acid: a new pharmacological tool for retina research. *Science* **211**, 182–185.

Stone J & Fukuda Y (1974). Properties of cat retinal ganglion cells: a comparison of W-cells with X- and Y-cells. *J Neurophysiol* **37**, 722–748.

Takahashi JS, DeCoursey PJ, Bauman L & Menaker M (1984). Spectral sensitivity of a novel photoreceptive system mediating entrainment of mammalian circadian rhythms. *Nature* **308**, 186–188.

Trevino SG, Villazana-Espinoza ET, Muniz A & Tsin AT (2005). Retinoid cycles in the conedominated chicken retina. *J Exp Biol* **208**, 4151–4157.

Tu DC, Zhang D, Demas J, Slutsky EB, Provencio I, Holy TE & Van Gelder RN (2005). Physiologic diversity and development of intrinsically photosensitive retinal ganglion cells. *Neuron* **48**, 987–999.

Warren EJ, Allen CN, Brown RL & Robinson DW (2003). Intrinsic light responses of retinal ganglion cells projecting to the circadian system. *Eur J Neurosci* **17**, 1727–1735.

Wong KY & Berson DM (2005). Bipolar and amacrine inputs modulating ganglion-cell photoreceptors. *Association for Research in Vision and Ophthalmology* Abstract no. 2332.

Wong KY, Cohen ED & Dowling JE (2005*a*). Retinal bipolar cell input mechanisms in giant danio. II. Patch-clamp analysis of on bipolar cells. *J Neurophysiol* **93**, 94–107.

Wong KY & Dowling JE (2005). Retinal bipolar cell input mechanisms in giant danio. III. ON-OFF bipolar cells and their color-opponent mechanisms. *J Neurophysiol* **94**, 265–272.

Wong KY, Dunn FA & Berson DM (2005*b*). Photoreceptor adaptation in intrinsically photosensitive retinal ganglion cells. *Neuron* **48**, 1001–1010.

Yoshimura T & Ebihara S (1996). Spectral sensitivity of photoreceptors mediating phase-shifts of circadian rhythms in retinally degenerate CBA/J (rd/rd) and normal CBA/N (+/+) mice. *J Comp Physiol [A]* **178**, 797–802.

Zhang DQ, Stone JF, Zhou T, Ohta H & McMahon DG (2004). Characterization of genetically labeled catecholamine neurons in the mouse retina. *Neuroreport* **15**, 1761–1765.

Zhang DQ, Zhou TR & McMahon DG (2007). Functional heterogeneity of retinal dopaminergic neurons underlying their multiple roles in vision. *J Neurosci* **27**, 692–699.

Acknowledgements

We thank Valerie Maine for performing the retrograde labelling of ipRGCs. This work was supported by a Ruth L. Kirschstein National Research Service Award training grant (1 F32 EY016678-01) awarded to K.Y.W and by NIH grant R01 EY12793 to D.B.